DAMAGE TOLERANCE EVALUATION OF FIBER REINFORCED COMPOSITE TAIL ROTOR BLADES

Elif Ahci
EUROCOPTER Germany GmbH
81663 Munich, Germany

Abstract

The dynamically loaded structures of helicopter rotor systems have to be evaluated and substantiated according to the American or European rules of the FAA or JAA. Main and tail rotor blades, which mainly consist of composite materials, are the most prominent examples of such structures.
During the last decades EUROCOPTER Germany has developed and substantiated various composite parts of different helicopters towards simplification, improved reliability, increased life, lower weight and reduced service and maintenance costs. The BO105 and EC135 helicopters were certified according to FAR 27 and JAR 27 "Small Rotorcraft". The BK117 and the newest version of the BK117, the C-2 (EC145) was certified according to FAR 29. As the certification authorities demand for an improved damage tolerant behavior, especially for dynamically loaded structures, basic damage tolerance material data were studied. Considering the substantiation efforts performed on the various composite parts of the different helicopters, there is a need for a new unified certification rule and advisory material to be issued for composite helicopter components.
This paper basically describes the damage tolerance evaluation of the fiber reinforced composite BK117 C-1 tail rotor blades according to the proposed new rule. The need for a new rule and the proposed rule itself are explained first. Then, development of basic fatigue and damage tolerance data at material and component levels is described. Finally, damage tolerance analysis and determination of inspection intervals for composite tail rotor blades are presented in detail.

TABLE OF CONTENTS

1 INTRODUCTION 1
2 GENERAL CERTIFICATION REQUIREMENTS AND DAMAGE TOLERANCE PRINCIPLES 2
2.1 General Substantiation Principles 2
2.2 Proposed New Rule 3
3 BK117 C-1 TAIL ROTOR BLADE TECHNOLOGY 3
4 BASIC STRUCTURAL BEHAVIOUR OF TAIL ROTOR BLADES 5
5 ESTABLISHMENT OF BASIC MATERIAL FATIGUE AND DAMAGE TOLERANCE DATA 6
6 DAMAGE TOLERANCE ANALYSES OF COMPOSITE TAIL ROTOR BLADES 7
6.1 Damage Tolerance Tests 7
6.1.1 Demonstration of Limit Load Capacity 10
6.2 S-N Curve Establishment 10
6.3 Determination of Inspection Intervals 12
7 QUALITY ASSURANCE METHODS APPLIED TO TAIL ROTOR BLADES 13
8 CONCLUSION 13
9 REFERENCES 14

1 INTRODUCTION

On June 13, 1979 the first flight of the BK117 of MBB Helicopter Division - now EUROCOPTER Germany (ECD) - took place. The BK117 was co-developed with Kawasaki Heavy Industries of Japan, who was responsible mainly for design and manufacturing of the center fuselage, main gearbox and electrical system as well as fuel tank design. Since 1979, about 475 helicopters are flying worldwide. The tail rotor system of this helicopter is similar to light twin helicopter BO105 except the rotor blade design which includes a different geometry but mainly comparable glass/epoxy composite materials. The helicopter family BO105, BK117 (Figure 1) and the newly developed BK117 C-2 (EC145) is equipped with a hingeless main rotor system. But it should be noticed that new materials and continuous improvements were introduced during the detailed design over 35 years in recent developments.

Figure 1: Multi-purpose helicopters BK117 C-1

In the 90's, further improvements such as glass cockpit technology and aerodynamic optimized fuselage shaping, along with the use of composite material and new fabrication methods - not mentioning other design features - led to development of the light twin EC135 [1] as successor to the BO105. As a logical step, the BK117 C-2 (EC145) now follows to satisfy market demands of the new century by taking the best technology available from EC135 and BK117, and providing customers a state-of-the-art technology medium twin helicopter meeting their requirements for present and future operations [2].
All versions of the BK117 are equipped with the semi-rigid tail rotor with 2 twisted glass fiber reinforced blades with erosion protection strip (Figure 3). The version C-1 is however equipped with the tail rotor blade, the width of which is slightly higher and generates higher thrust compared to that of BK117 former versions A-3, A-4 and B-2. These blades were manufactured by prepreg composite materials. Further information about the tail rotor blade design is given later in this paper.

2 GENERAL CERTIFICATION REQUIREMENTS AND DAMAGE TOLERANCE PRINCIPLES

2.1 General Substantiation Principles

In the past, all helicopters have been designed to safe-life requirements. The majority of the dynamically loaded structures of helicopters are substantiated based on Safe Life procedure. The Safe Life of a helicopter component is the service time in flight hours that will preclude the initiation of fatigue cracks. As derived and stated in the Helicopter Design Guide [3], the Safe Life is calculated using the usage spectrum, in-flight-measured loads, and the reduced fatigue strength (i.e. working curve) determined from full-scale fatigue testing of as-manufactured components. The Safe Life approach mainly leads to replacement times. The Safe Life evaluation method differs from one helicopter manufacturer to another because of the differences in the individual parameters influencing the final product. Determination of Safe Life requires consideration of other sources of randomness besides fatigue strength-such as usage spectrum, flight loads, and damage accumulation (Miner's Rule). The Safe Life does not account directly for such events as the presence of cracks due to manufacturing, maintenance, environment, or discrete damage. Therefore, the reliability of the Safe Life could be lower than calculated if the combined probability of the above mentioned events is of the same order as the probability of having a fatigue crack. Nevertheless, the reliability of safe-life components can be increased by lowering their replacement times or decreasing their usage. Thus, the Safe Life approach has generally been proven to be adequate. However, there have been a number of field problems with cracking components, which lend themselves to the application of a damage tolerance approach.
In recent years the orientation in helicopter industry is more transitioning to damage/flaw tolerance philosophy. Introduced in October 1989, FAR 29.571 at Amendment 28 requires damage/flaw tolerance substantiation for transport category helicopters. The requirements of fatigue substantiation under §29.571 were reviewed later by the authorities and flaw-tolerant safe-life and fail-safe-evaluation concepts were included in FAR 29.571 as Amendment 40 (Figure 2) [4].

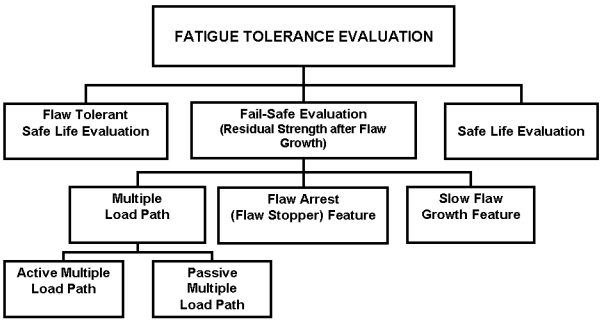

Figure 2: Fatigue evaluation of transport Category rotorcraft structures (Including Flaw Tolerance) according to FAR29.571

Damage tolerance of a helicopter component is ensured by inspection or part removal before a crack grows critical. The inspection interval or removal time is calculated for the assumed crack using the usage spectrum, flight-measured loads, and the material crack growth data. The crack growth analysis results are verified by the laboratory evaluation of the cracked components, and if necessary by the additional crack growth testing of the field-returned components with cracks or the pre-cracked components. The damage tolerance starts where the Safe Life ends, i.e., when there is a crack; it also accounts for events not covered by the Safe Life, such as cracks caused by manufacturing, maintenance, environment, or discrete damage.
In EUROCOPTER, the BO105, EC130 and EC135 were certified according to Joint Aviation Requirements JAR27 'Small Rotorcraft'. The BK117 and the newest version of the BK117, the C-2 (EC145), were certified according to FAR 29.571. However, as the primary structure of these helicopters includes composite materials, the German airworthiness authority Luftfahrtbundesamt (LBA) issued a Special Condition 'Primary structures designed with

composite material' that had to be fulfilled additionally [5]. Therefore, for all composite components such as main rotor blades, Amendment 40 together with special conditions issued specifically for composite structures were applied in the certification program. The special condition addresses subjects like:

- Demonstration of ultimate load capacity including consideration of manufacturing and impact damages
- Investigation of growth rate of damages that may occur from fatigue, corrosion, intrinsic defects, manufacturing defects or damages from discrete sources under repeated loads expected in service
- Consideration of the effects of environmental conditions and material variability
- Substantiation of bonded joints

The modified tail rotor blades of BK117 C-2 (EC145) were certified according to Amendment 16. Then, these modified blades were adapted to BK117 C-1 helicopters too. The remaining BK117 C-1 prepreg tail rotor blades are recertified by following the principles of the proposed new rules. The proposed rules follow the current laws §29.571 including the special conditions of LBA.
For the dynamically loaded EC145 and EC135 rotor blades and the EC135 fenestron drive shaft, the Flaw Tolerant Safe Life method is used for substantiation. In addition, fail-safe features were incorporated into the design to ensure sufficient residual strength capability after flaw growth.

2.2 Proposed New Rule

As the present fatigue tolerance law FAR 29.571 does not clearly state the necessary substantiation steps for the composite structures, several "special conditions" were established by the different certification authorities. Subsequently, the new rule "Damage Tolerance and Fatigue Evaluation of Composite Rotorcraft Structure FAR 27.573/29.573" has been proposed by taking into account the knowledge of the industry and the certification authorities. The strength of principal composite structural elements or components must show that catastrophic failure due to static and fatigue load requirements, considering the intrinsic/discrete manufacturing defects or accidental damage, will be avoided throughout the operational life or prescribed inspection intervals of the rotorcraft. For each element identified, inspection intervals and replacement times must be established as necessary to avoid catastrophic failure. Replacement times must be demonstrated by tests or by analysis supported by tests, to ensure that the structure is able to withstand the repeated loads of variable magnitude expected in service. In establishing these Replacement Times (Flaw Tolerant Safe Life), the following items must be considered:

- Damage identified by threats
- Maximum acceptable manufacturing defects and service damages
- Ultimate load strength capability must be shown after application of repeated loads

However, for the determination of Inspection Intervals, the minimum required residual strength is the limit load. Inspection intervals must be established to ensure that any damage identified that may occur from fatigue and/or other in-service causes will be detected before it has grown to the extent that the required residual strength capability cannot be achieved.
BK117 C-1 tail rotor blade is taken as an example for the substantiation of a composite structure following the principles of the proposed new rule which goes along also with the current rule §29.571 and special conditions. As a result of this work the inspection intervals are defined. The details of this work are explained in the following pages.

3 BK117 C-1 TAIL ROTOR BLADE TECHNOLOGY

The BK117 tail rotor blades are based over a decade of experience with composite materials. The tail rotors in all versions of BK117 are the two bladed teetering semi rigid types of new technology with erosion protection strips (Figure 3). The version C-1 is however equipped with a tail rotor blade the width of which is slightly higher and generates higher thrust compared to that of BK117 former versions A-3, A-4 and B-2. Main Characteristics of the BK117 C-1 tail rotor blade is given in Table 1. Version C-1 tail rotor blade is of a new design compared to that of BO105 which uses a MBB developed advanced cambered airfoil with a thickness ratio of 8%. This airfoil ensures a much higher tail rotor thrust capability than the standard blades. It is a light weight construction manufactured of E-Glass/Epoxy prepreg, using a similar design to that of the main rotor blade.

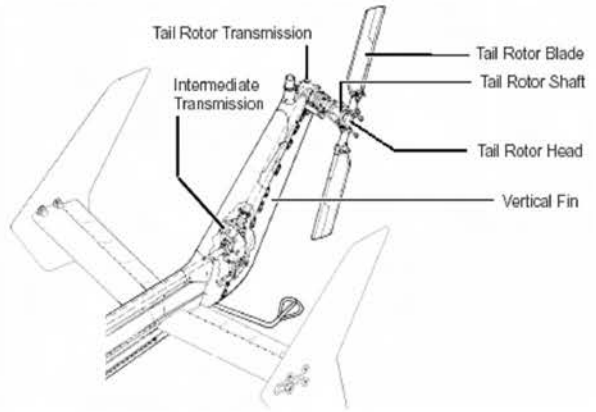

Figure 3: Tail unit components

	BK117 C-1 TRB	BK117 former TRBs
Weight Distribution- [kg/m]	1.24	1.17
Flap Bending Stiffness [Nm^2]	323	288.7
Lead-Lag Bending Stiffness [Nm^2]	48320	43717
Torsional Stiffness [Nm^2]	464.4	205.5
Blade Width [mm]	220	200 (20 mm tab)
Profile	S102E	S102E
Control Axis- % width	26.5	23.8
Center of Gravity-% width	28	27.8
Elastic Center- % width	27.1	23.9

Table 1: Comparison of cross section and profile characteristics of former and BK117 C-1 tail rotor blades

The blade has a rectangular shape with a trapezoidal root. The outer end of the blade is formed by a curvature. The cross-section is designed asymmetrically (Figure 4). The blades are attached to the tail rotor head via the blade mounting forks. Two steel bushings are molded into the blade root and form the blade fitting. Reinforcing prepreg glass rovings are looped around them. The blades are each retained by two fitted bolts, which have a narrow thread extension for the balancing weights.

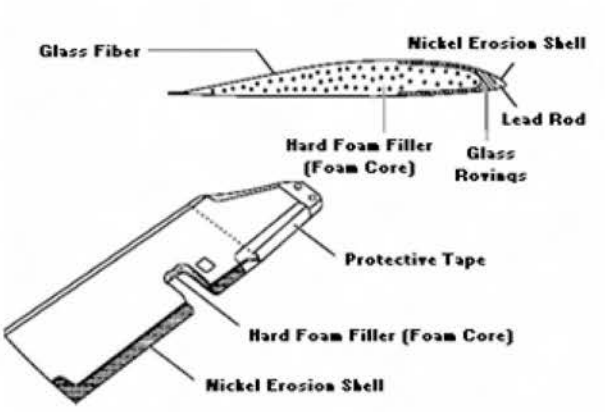

Figure 4: Location of externally bonded blade components and cross sectional view

The tail rotor blade consists of blade core and external blade components. The blade core consists of a C-spar, made of unidirectional prepreg glass roving, and a support core, made of hard foam. The nose of the C-spar contains a lead rod. The prepreg skin is made of glass fiber reinforced plastics (GRP). The nickel strip with an integrated tip cap prevents leading edge erosion. It is bonded after blade curing. The inner leading edge and the inner trailing edge are protected with a GRP cap. Additionally a protective tape is bonded to the inner leading edge to protect against unfavorable environmental conditions. The entire blade surface is painted with a polyurethane varnish (Figure 5).

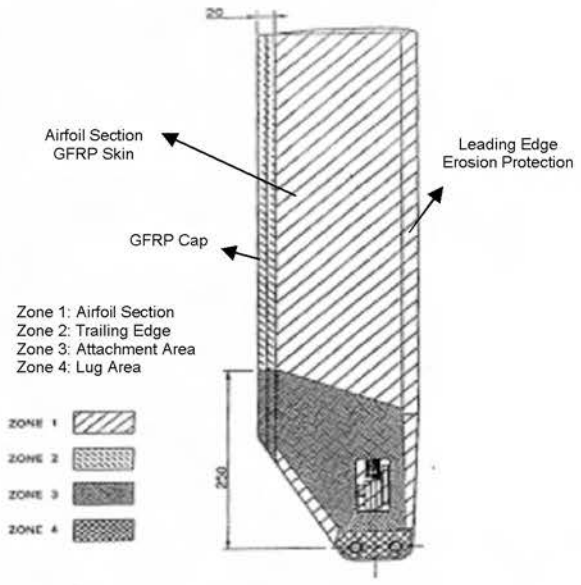

Figure 5: Sketch of the BK117 C-1 tail rotor blade with different zones.

4 BASIC STRUCTURAL BEHAVIOUR OF TAIL ROTOR BLADES

A finite element examination has been carried out for the design and damage tolerance analyses of the composite tail rotor blades. For this purpose, a two-dimensional finite element (FE) program called SABINA [6] developed in EUROCOPTER was utilized. This ECD own code computes the six different stiffnesses of the cross sections in three coordinate directions. Additionally it also calculates the normal and shear stress distributions for any load combination. In general, the finite element analysis by SABINA yields good results. However, it is important to keep in mind that the cross sections are assumed to be constant over a great length. Therefore, in order to determine additional stresses due to strong cross section variations or special load introduction areas, analyses are aided by special tools and calculation procedures.
As a result of the computational work, the cross sectional characteristics of the tail rotor blades were calculated at various radius stations. Stress analyses were conducted simultaneously with an experimental program to determine the most critical cross section on the blade. After the experimental observations (will be explained in detail later) and stress analyses, it was concluded that the cross section measured at 30 mms from the bolt center is the most critical (Figure 6) area. As a consequence of the resulting high stresses, skin cracks initiate at this cross section (Figure 7).

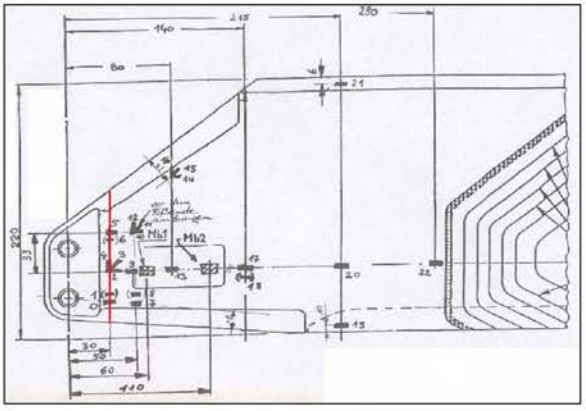

Figure 6: Sketch of the tail rotor blade showing certain dimensions including the critical cross section r = 30 mm.

Figure 7: Crack initiation and propagation at the blade skin of the bending test specimen after dynamic loading (at critical cross section r ≅ 30 mm).

The resulting stresses and strains at the critical section were determined by cross sectional FEM analyses as mentioned above (Figure 8). In this analysis, the effect of applied loads on resultant stress and strain fields (i.e. centrifugal force, vertical shear forces, flapping and lead-lag moments) was investigated individually and in combination (Figure 9). As a result of this analyses supported by component tests, it was found that the lead-lag/flap load combination (i.e., lead-lag and flapping bending moments) is the most critical loading for the BK117 C-1 tail rotor blades and results in high strains in axial direction. Subsequently, a surface crack initiates in the blade skin at the critical radius location r ≅ 30 mm (Figure 6 and Figure 7) as a result of this normal strains.

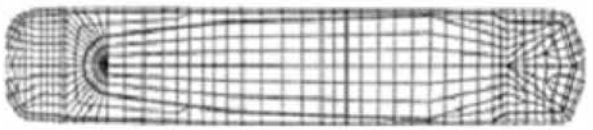

Figure 8: Finite element mesh of the BK117 C-1 tail rotor blade cross section at r = 30 mm

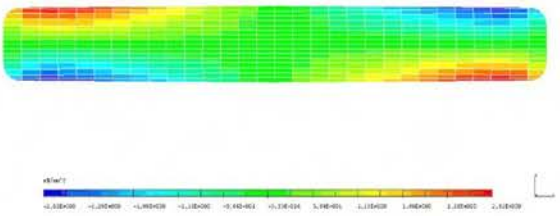

Figure 9: Resultant shear stress due to transverse shear force.

5 ESTABLISHMENT OF BASIC MATERIAL FATIGUE AND DAMAGE TOLERANCE DATA

The substantiation of the composite tail rotor blade and its behaviour in case of damage (e.g. skin cracks) existence was confirmed with regard to previously identified damage. This approach assumes a number of elementary tests, which form a pyramidal hierarchy (Figure 10) ranging from basic coupon tests to tests on full-scale blades with manufacturing or in-use damages [7].

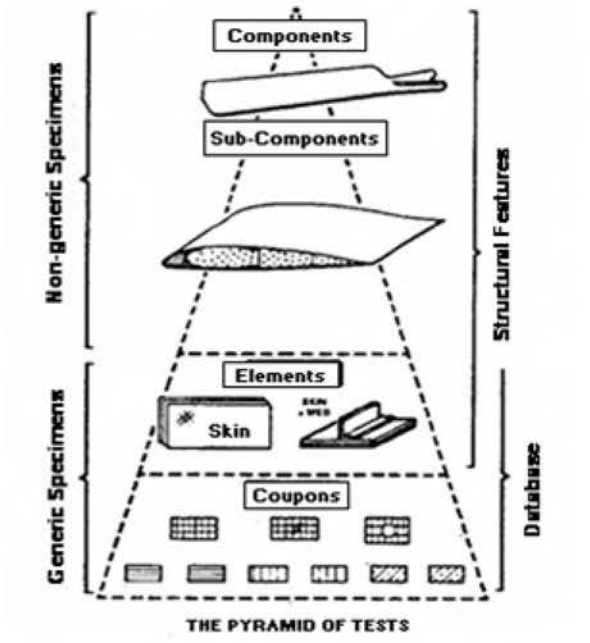

Figure 10: Building block approach-Test Pyramid

The generic, i.e. general characterization, tests were performed at ECD. The material stiffness and strength properties of the fiber composite materials used for tail rotor blades were measured with the help of standardised coupon tests. BK117 C-1 tail rotor blade skin is made up of quasi-isotropic E-Glass/913 prepreg with 47% fiber volume ratio. The basic stiffness and strength values for bending and shear responses were determined by using the long and short unidirectional beam coupons (Figure 11).

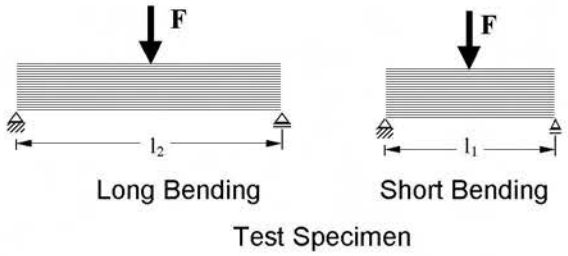

Figure 11: Basic static structural tests

The dynamic characterization of quasi-isotropic material system was performed by fatigue tests with Amsler type shear coupons and Schenk type bending coupons at various stress ratios. In Figure 12, the WEIBULL mean curve and working curve for quasi isotropic E-Glass/913 material system at stress ratio R = 0.2 determined from bending tests is given as an example. Corresponding Goodman diagram for the same material system is given in Figure 13. The mean and working curves are described by the four parametric WEIBULL formula:

$$\sigma_o = \sigma_\infty + \frac{\sigma_{ult} - \sigma_\infty}{e^{\left[\left(\frac{\log N}{\alpha}\right)^\beta\right]}}$$

with:

σ_o: Upper Stress
σ_{ult}: Ultimate stress value
σ_∞: Endurance Limit
α, β: Curve parameters

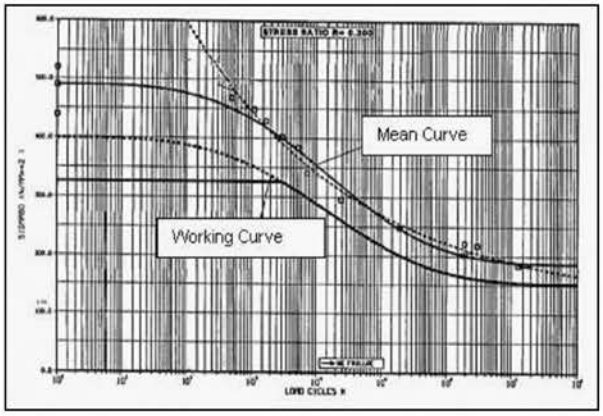

Figure 12: Four parameter WEIBULL mean curve and working curve formed from quasi-isotropic E-Glass/913 Schenck type bending coupon test results (R = 0.2)

	σ_{ult} [MPa]	σ_∞ [MPa]	α [-]	β [-]
WEIBULL Curve	490	187	4.63	3.63
Working Curve	399.5	152.5	4.63	3.63

Table 2: Parameters of WEIBULL mean and working curves

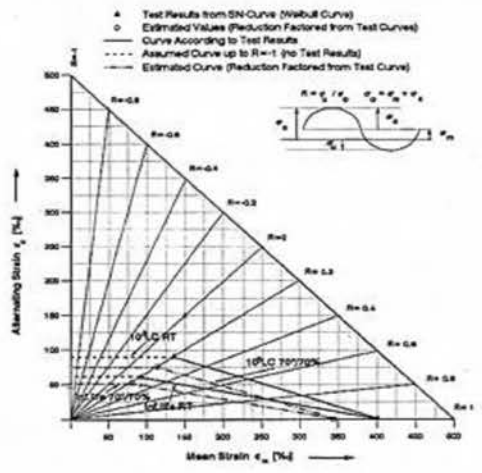

Figure 13: Goodman diagram of quasi-isotropic E-Glass/913 (Probability of confidence = 95%, Probability of survival = 99.9%)

6 DAMAGE TOLERANCE ANALYSES OF COMPOSITE TAIL ROTOR BLADES

6.1 Damage Tolerance Tests

The tail rotor blades were fatigue tested in order to get information about the fatigue strength of the attachment area and of the skin zone. A comprehensive test program ranging from conventional Safe Life limit tests to damage propagation tests were applied to achieve this purpose and to obtain data for damage tolerance analyses.

For the fatigue tests constant axial load simulating the centrifugal force, alternating flapwise and chordwise bending moments as well as torsional moments were applied, simulating the loading conditions in service. After the fatigue tests residual strength tests had to be performed. Limit load capacity was proven at this point. For this purpose, the static tests were performed to get information about the loading capacity of the attachment area. In static limit load capacity tests (residual strength tests), the influence of the high temperature and moisture had to be taken into account according to the proposed new rule in line with special conditions of the LBA issued for composite structures. Therefore, static component tests were performed at room temperatures with the loads increased by the hot/wet degradation factors. The maximum loads were simultaneously applied to cover the worst case possible.

Table 3 summarizes the process for the component tests that take into account the requirements of the new rule and special condition issued by LBA. These tests are the basis for the life calculations.

1. Component specimens
   - Specimens with intrinsic, manufacturing and/or impact damages
2. Tests
   - Separate component tests for critical area
   - Constant amplitude tests at different loads
   - Test monitoring
   - Documentation of: Type of damage
     Damage begin
     Size
     Location
     Growth rate
3. Residual strength test with pre-damage specimens after fatigue test
   - Proof of Limit Load capacity
   - Load amplification factor to simulate hot/wet conditions

Table 3: Process of the component tests

Several tail rotor blades were subjected to complex loading of centrifugal force, flapping and lead-lag and torsional moments. Basically two types of tests were performed:

- Tests with long specimens to test the skin region
- Tests with short and middle length specimens to test the attachment area including the critical section (r = 30 mm)

The resultant dynamic forces were introduced in a test set-up by the four hydraulic cylinders (Figure 14). The test loads were applied to the tip of the blade.

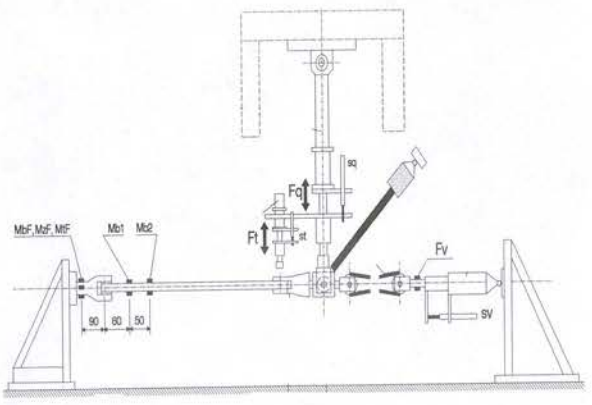

Figure 14: Sketch of the test set-up used for static and dynamic testing of BK117 C-1 tail rotor blades

In order to make application of the test loads possible, one end of the blades was reinforced with glass fiber laminates (Figure 15). This avoids the fracture emanating from the adapter through which the test loads are induced. Figure 15 shows a bending test specimen in its upper test position. It is pretensioned by a centrifugal force of about 33 kN and simultaneously loaded by flapping and lead-lag moments. At the right side the blade attachment area is clamped into a fork simulating the rotor hub. This test mainly simulates the load conditions between blade attachment and 'flapping hinge'.

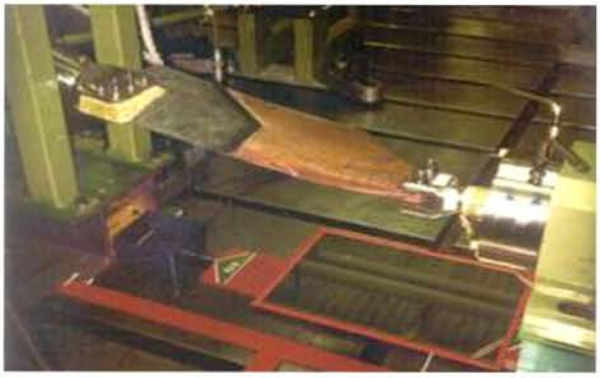

Figure 15: SN219 tail rotor blade specimen loaded by bending moments and centrifugal force

The tail rotor test blades were instrumented with strain gauges for determination of the bending moment distribution (Figure 18). After the early regular lifetime tests at different load levels, crack initiation was observed after certain number of load cycles at the attachment area in the blade skin, around 30 mm distance from the center of bolts (r = 30 mm). Additional tests were performed on blades with and without cracks to examine this phenomenon in more detail. Since bending is the critical loading at the attachment area, medium length (580 mm) bending test specimens were used in these tests. Test blades were subjected to constant axial force representing the centrifugal load combined with alternating flap and lead-lag moments. Strains were measured by attached strain gauges to various cross sections along the blade to determine the influence of each load (centrifugal force, flapping moment and lead-lag moment) on the resulting strain especially at the critical section (Figure 16).

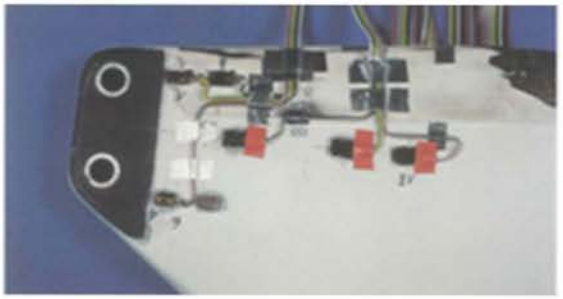

Top surface

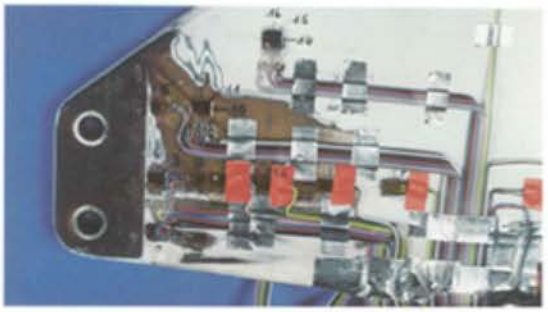

Bottom surface

Figure 16: Tail rotor blade with strain gauges attached to top and bottom surfaces

The component tests were started with an application of only centrifugal force; this was followed by a combined application of centrifugal force and flapping moment; and consequently centrifugal force and lead-lag moment in static mode. After static part, dynamic loading starts. In dynamic part applied loads were increased gradually to final value and cyclic loading follows afterwards. Any type of visible changes such as skin cracks, delaminations emerge in the blade structure was recorded during the test. The type of damage, beginning of first damage, damage size and location and finally the growth rate of damage were documented during the tests.

As a result of the observations concerning the damage initiation and evolution, it was discovered that the damage first occurred in the form of a skin crack in the blade skin at the attachment area approximately 30 mm distance from the bolt center ($r \cong 30$ mm). Hence, the cross section at $r \cong 30$ mm was decided as the most critical in terms of damage initiation and resulting highest normal strains. This examination showed that the damage tolerance behavior of the BK117 C-1 tail rotor blade is mainly dictated by the bending strength of the quasi-isotropic composite material of the blade skin.

In Figure 17, crack in the blade skin at attachment area of the SN219 test specimen is shown after 22000 and 38700 load cycles. The test specimen was subjected to 33 kN constant centrifugal force, 400±400 Nm flapping moment and ±380 Nm lead-lag moment. The first visible damage was a skin crack initiating from the rear side of the blade's

bottom surface close to the neck shell. This crack was noticed after approximately 5500 load cycles. An increase in the number of cycles resulted in propagation of the crack through the surface of the blade in a 45° angle (with respect to the blade axis) towards the identification label as shown in Figure 17. When the crack reached the proximity of the leading edge and crunching sounds were increasingly audible, dynamic loading was stopped and limit load test was performed. Same procedure was repeated with the other test blades.

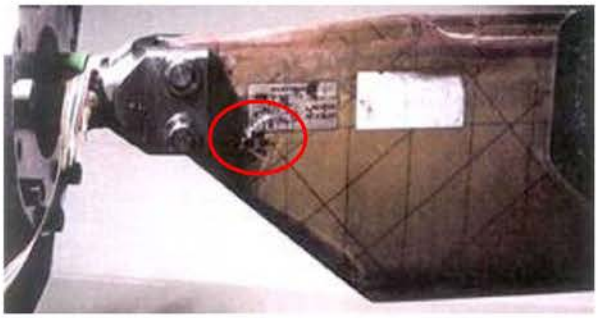

(a) Skin crack after 22000 load cycles

(b) Skin crack after 38700 load cycles

Figure 17: View from the bottom side of SN219 test blade after dynamic loading

In addition to the tests with previously undamaged blades, i.e., blades without any initial damage, supplementary tests were performed with the pre-damaged blades, i.e., blades with initial damages (Figure 18).

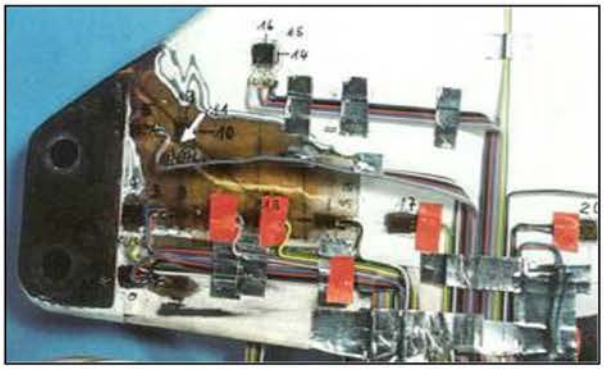

Figure 18: SN139 tail rotor blade with 40 mm initial crack before dynamic testing

The crack growth on the blade skin was visually observed during the component tests. For the type of damages that were not possible to monitor visually, computed tomography was used to detect and follow the damage growth. Figure 19 shows the process of crack propagation reporting overtime throughout the test.

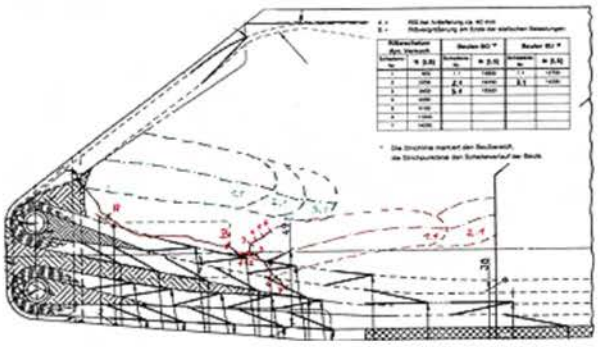

Figure 19: Sketch of the damage propagation on SN219 tail rotor blade during dynamic loading

In Figure 20, the result of the crack growth analyses performed by using the test data is presented. One of the components depicted in this figure was from service and had already a crack at the beginning of the test (Figure 18). As seen in the figure, the crack propagation rate is not very much different for the components shown. The first visible crack appeared earlier on SN219 than SN391. The time that the crack took to propagate after its origination is longer than the time necessary for the initiation of the crack itself. The test data from these component fatigue tests were used as basis for the calculation of inspection intervals. In addition to the first detectable crack data, the limit load capacity of the blades has to be determined as well, to calculate the inspection intervals.

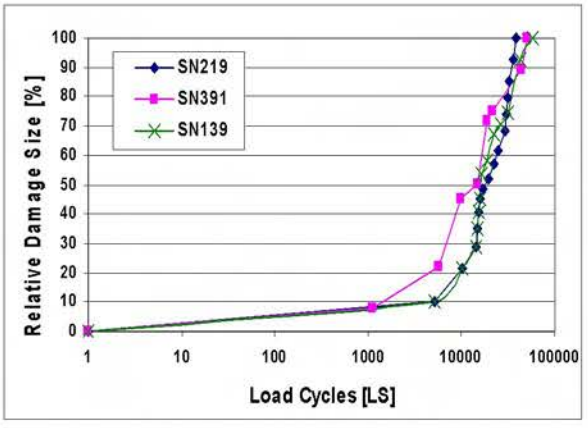

Figure 20: Crack growth at bottom side of BK117 C-1 tail rotor blades for test components SN219, SN391 and SN139

6.1.1 Demonstration of Limit Load Capacity

After the fatigue tests, residual strength tests were performed. Limit load capacity was proven by these tests including the load amplification factors to simulate the hot/wet conditions. The residual strength tests (i.e. limit load capacity tests) were performed on predamaged blades after dynamic loading. The evaluation following these tests should show that the residual strength of the predamaged structure is equal to, or greater than the strength required for the specified design loads. The limit load capacity tests showed that the predamaged blades were able to withstand critical limit flight and ground loads, considered as ultimate loads, with the extend of damage tolerance evaluations.
Figure 21 shows a BK117 C-1 test blade in a limit load application. In this specific example, the SN219 test blade was subjected to limit loads after 39970 load cycles. Constant centrifugal force was applied simultaneously with flapping and lead-lag moments in limit load tests. No major expansion in the existing damage state was observed.

Figure 21: Test sample in test rig at limit load test (F_V= 33kN, M_{bBolt}= 800Nm, M_{zBolt}= -934Nm, limit loads including a factor of 1.3 for temperature and humidity)

The status of damage after limit load capacity tests is shown with two sample photos in Figure 22. It can be seen from the figure that there was no major expansion in the damage state or failure of the blade structure after the limit load tests.

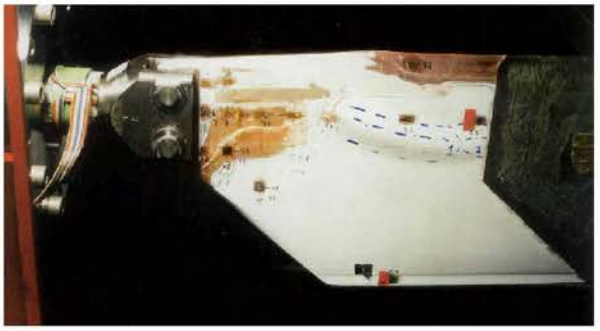

(a) SN219 test blade after limit load application

(b) SN391 test blade after limit load application

Figure 22: BK117 C-1 tail rotor blade test specimens after limit load tests

6.2 S-N Curve Establishment

The lifetime evaluation of the dynamically loaded tail rotor blades is carried through with working S-N curves based on component test results and/or analyses and the load spectra determined from flight load measurements.
All types of S-N curves are based on fatigue test results at different stress levels but with a constant stress ratio R. This stress ratio should be chosen to correspond with the predominant stress ratio of the component tests. Therefore, the dominant value of R = 0.11 was chosen as the stress ratio value in this study.
In order to characterize fatigue test data by means of an analytical expression, the WEIBULL formula can be used successfully to describe the fatigue behavior in the low cycle as well as in the high cycle region. The four parametric WEIBULL curve allows the strength description of a component in the entire range from the static strength to endurance limit. Due to this advantage the WEIBULL curve is the standard S-N curve type used at EUROCOPTER, Germany. The WEIBULL curve is defined for a constant stress ratio R (= max. stress value / min. stress value) by the following formula (for amplitude loads):

$$M_a(N) = M_{a_\infty} \frac{M_{a_{ult}} - M_{a_\infty}}{e^{\left[\left(\frac{\log_{10} N}{\alpha}\right)^\beta\right]}}$$

with: M_{a_∞} : Endurance limit amplitude

$M_{a_{ult}}$: Ultimate strength amplitude for stress ratio R determined as

$$M_{a_{ult}} = M_{ult} \frac{1-R}{2}$$

M_{ult} : Ultimate strength

α, β : WEIBULL parameters

The four parameters of the WEIBULL curve are determined by using a non-linear regression analysis [3]. These parameters (i.e. the form of WEIBULL curve) depend on the number of test points, the distribution of the test points and availability of supporting data. The supporting data preferably comes from S-N curves of similar components or S-N curves and HAIGH diagrams of coupon tests or materials. The material S-N curve, representing the fatigue behaviour of blade skin material (Figure 12) was used as supporting data in this study. In addition, the fatigue behaviour of similar material systems was examined to determine the WEIBULL mean curve parameters.

The mean S-N curve corresponds to a survival probability and confidence level of each 50%. The working curve is derived from the mean curve and corresponds to a survival probability of 99.9% and a confidence level of 95%. A reduction factor is applied to mean curve to calculate the working curve. This reduction factor accounts for the variability of the component strength and depends on the several factors such as number of tests, the standard deviation of the results etc.

Following the methodology explained above, the working curves were created with measured strain values at the critical area (i.e. highest loaded area). The rear corner of the blade bottom surface, at r = 30 mm is the most critical area for the BK117 C-1 tail rotor blades. Therefore, the strains calculated at this critical area were used in S-N curve establishment. For this purpose, a relationship between the applied loads, such as centrifugal force, flapping and lead-lag moments, and the strains at the critical section was developed. The strain-force relationship basically gives the strain values at the critical section in terms of applied forces and moments in the tests. The input loads in the fatigue tests were defined at the bolt position (i.e., r = 0 mm). So, to derive this relationship, first conversion factors were derived to correlate the moments and forces defined at the bolt position to those at the critical section. Then, a second set of factors was defined to convert the moments and forces to strains at the critical area. The general form of this relationship can be expressed as follows:

$$\varepsilon_{r=r_{critical}} = aM_{\beta,B} + bM_{\zeta,B} + c \qquad (1)$$

with: $\varepsilon_{r=r_{critical}}$: Strain at the critical section,

$M_{\beta,B}$: Flapping moment defined in the test procedure at bolt position,

$M_{\zeta,B}$: Lead-lag moment defined in the test procedure at bolt position,

a, b : Conversion factors,

c : Constant strain due to centrifugal force.

After determining the relationship between the strains and the applied loads, the test loads were converted to the strains at the critical area for each component fatigue test. Then, WEIBULL mean and working curves representing the fatigue behavior until the first crack initiation and up to limit load capacity were established. These curves were created by using the conventional full scale fatigue test results, first alone and then in combination with the test points representing the first crack initiation and limit load capacity of the blades, i.e. Strain-Load Cycle data points at which the first detectable crack was observed and limit load application was performed. Figure 23 shows an example WEIBULL mean and working curves representing first crack initiation in the blade skin.

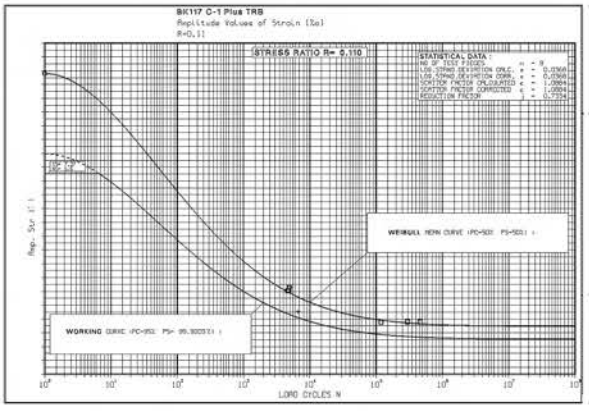

Figure 23: WEIBULL Mean curve and Working curve representing the first detectable crack for BK117 C-1 tail rotor blade (R=0.11)

The load spectrum was derived from flapping and lead-lag moments measured in flight with strain gauges attached to critical measurement points for moments along the tail rotor head assembly. So, the measured moments at these positions had to be converted to the strains at the critical area. Flight test measurements give a normalized load spectrum for various radius locations. Normalization is made based on an assumption of a 1 m deflection at the blade tip. The relation between the moments at the measurement positions and at the tail rotor blade bolt (r = 0) was estimated through conversion factors derived by using the normalized in flight measurements.
Subsequent to the determination of the load spectrum and the working S-N curve, the fatigue life of a tail rotor blade until the first crack initiation and up to the limit load capacity was evaluated. Lifetime determination by using the working curve is usually used for replacement time calculations.
In lifetime calculations, the damage due to ground-air-ground load cases was determined according to Minor's rule and then added to the flight load damage. The unbiased measured load matrix (Rainflow matrix) was used to calculate the damage ratios for each element of the Rainflow matrix. The summed up damage ratio allows the fatigue life calculation according to Miner's linear cumulative damage hypothesis. On the other hand, the working load spectrum for the flight load cases (i.e., high cycle load cases) is based on an approximated load spectrum (i.e. lognormal load distribution). In this case, a mean stress correction was carried out for each amplitude load class. Then, corrected mean S-N curve and load cycles from the lognormal curve were used to determine the damage ratios. Finally, by adding up the damages determined for both load cases, the fatigue lifetime was calculated. As a result of the analyses lifetime until the initiation of first visible crack was determined as 940 hours. Similarly, lifetime representing the duration up to limit load capacity was determined as 2050 hours.

6.3 Determination of Inspection Intervals

Inspection intervals must be defined so that after the damage initially becomes detectable by the inspection method specified, the damage will be detected before it exceeds the extent of damage for which residual strength is demonstrated. Therefore, inspection intervals were defined in accordance with this special condition. The philosophy of calculation of the inspection intervals is shown graphically in Figure 24 .

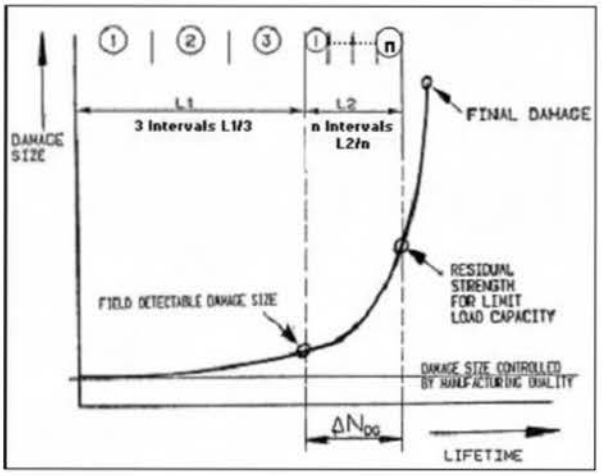

Figure 24: An example sketch showing the change of damage size with respect to lifetime and basics of inspection interval determination

Using the special conditions as a guideline, the time period until the first detectable damage (i.e. the skin crack initiating at the rear corner of the blade bottom surface around r = 30 mm) was divided into three intervals. Then, the time period from first detectable damage until limit load capacity was divided into "n" intervals. Usually, number 3 is used in EUROCOPTER Germany for the parameter "n". Then, based on these principles, the inspection times for these two intervals (so called L1 and L2 Figure 24) were determined. As a result of the calculations, for the new blades the first inspection has to be done after 300 hours. After the first damage initiation, the next and all following inspections have to be done also every 300 hours.
For the BK117 C-1 tail rotor blades, the first damage initiating in the blade structure is the crack in the prepreg skin. This crack is possible to be detected visually. Therefore, the inspections of BK117 C-1 tail rotor blades can be done visually after the defined intervals.

7 QUALITY ASSURANCE METHODS APPLIED TO TAIL ROTOR BLADES

Quality assurance checks are applied in order to assure that the quality of the test specimens used in the development and/or certification phases or for the quality assurance purposes correlates with the structural parts distributed to the customer. At EUROCOPTER Germany, computed tomography (CT) is used for the quality assurance of the rotor blades of BO105, BK117 and EC135 [8], (see Figure 25). Computed tomography was also used during the design phase of the BK117 C-2 tail rotor blades.

Originally, CT was developed for the medical field. To create a cross sectional image, an X-ray beam rotates around the object in a complete circle. Attenuation profiles of the beam are measured from several projection directions. With these data a computer calculates the image of the cross sectional slice having the thickness of the X-ray beam, about 1.5 mm. During the rotor blade examination cross section images are produced at various radius stations. When these stations are close to each other vertical and horizontal cuts in radial direction can also be computed.

CT is a very effective non-destructive testing (NDT) method to check the quality of fiber composite parts. Damages or defects like cracks or waves in the laminate of at least 0.2 mm size can be detected. By the determination of special CT numbers the local material density can be established. Thus, it can be checked if dark spots in a cross section consist of resin or critical air inclusions.

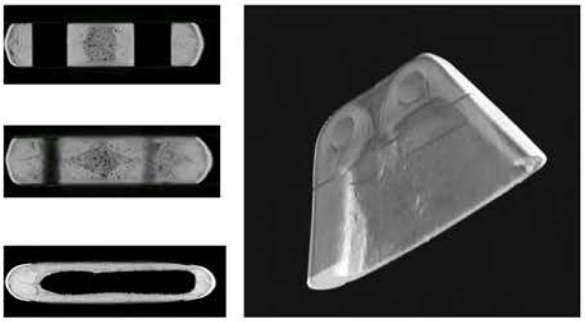

Figure 25: CT images of BK117 C-1 tail rotor blade

8 CONCLUSION

Throughout the past decades, the former helicopter division of MBB and now EUROCOPTER Germany has developed and substantiated various dynamically loaded composite parts towards simplification, improved reliability, increased life, lower weight and reduced service and maintenance costs. This development has become possible by using the exceptional qualities of the fiber reinforced composites with regard to strength and flexibility. Dynamic structures designed with the composite materials have an outstanding low crack growth and high fatigue strength. When these superior features of the composite materials are used together with the improved methods of the quality assurance, such as computed tomography (CT), remarkably reduced life cycle costs and improved structural safety for the helicopters can be achieved.

The damage tolerance evaluation study carried out for the fiber reinforced composite BK117 C-1 tail rotor blades was presented in this paper. The analyses were done by following the principles of the proposed new rule which is aligned with the old rule §29.571 and special conditions issued by the LBA. Throughout this study, an extended experimental work was performed to investigate the first damage initiation in the blades and limit load capacity of the composite blades. Ultimately, the inspection intervals were determined. With the proof of the limit load capacity and the possibility of establishing the inspection intervals with the help of first damage data, the damage tolerance substantiation for the BK117 C-1 tail rotor blades was demonstrated. This experience did provide us a solid basis for addressing the “damage tolerance” approach explained in detail by the proposed new rule concerning the fatigue substantiation of helicopter dynamic components.

9 REFERENCES

[1] Zwicker, C.: "*Configuration and Program Status of EUROCOPTER's New Light Twin Helicopter EC135*", 19th European Rotorcraft Forum, Cernobbio, September 1993

[2] Humpert, A.: "*Design, Development and Flight Testing of the new EUROCOPTER EC145 Medium Twin Helicopter*", 27th European Rotorcraft Forum, September 2001, Moscow

[3] Och, F.: "*Helicopter Fatigue Design Guide*", AGARDograph No 292, ISBN 92-835-0341-4, Nov. 1983

[4] Joint Aviation Requirements, JAR 29: Large Rotorcraft, Joint Aviation Authorities, Nov. 1993

[5] Bansemir, H., and Emmerling S.: "Fatigue Substantiation and Damage Tolerance Evaluation of Fiber Composite Helicopter Components", Applied Vehicle Technology Panel (AVT), Application of Damage Tolerance Principles for Improved Airworthiness of Rotorcraft; Corfu, Greece; 21-22 April, 1996

[6] Rapp, H.: "*New Computer Codes for Structural Analysis of Composite Helicopter Structures*", 17th European Rotorcraft Forum, Glasgow, September 1990

[7] AC 29-2C, Advisory Circular for the New Rule, Chapter 3: Airworthiness Standards transport Category Rotorcraft, February, 2002

[8] Oster, R.: "Computed Tomography as a Nondestructive Test Method for Fiber Main Rotor Blades in Development, Series and Maintenance", 23rd European Rotorcraft Forum, Dresden, Germany, September 1997